Article

Comparing natural gas leakage detection technologies using an open-source "virtual gas field" simulator

Chandler Kemp, Arvind P. Ravikumar, and Adam R. Brandt

Just Accepted

Comparing natural gas leakage detection technologies using an open-source "virtual gas field" simulator

[1] Chandler E. Kemp, Arvind P. Ravikumar, and Adam R. Brandt   *

Department of Energy Resources Engineering, 367 Panama Street, Stanford University, Stanford, CA 94305, USA

E-mail: abrandt@stanford.edu

Phone: +1-650-724-8251. Fax: +1-650-725-2099

[2] **Abstract**

[3] We present a tool for modeling the performance of methane leak detection and [4] repair programs that can be used to evaluate the effectiveness of detection technolo- [5] gies and proposed mitigation policies. The tool uses a two-state Markov model to [6] simulate the evolution of methane leakage from an artificial natural gas field. Leaks [7] are created stochastically, drawing from current understanding of the frequency and [8] size distributions at production facilities. Various leak detection and repair programs [9] can be simulated to determine the rate at which each would identify and repair leaks. [10] Integrating the methane leakage over time enables a meaningful comparison between [11] technologies, using both economic and environmental metrics. We simulate four ex- [12] isting or proposed detection technologies: flame ionization detection, manual infrared [13] camera, automated infrared drone, and distributed detectors. Comparing these four [14] technologies, we found that over 80% of simulated leakage could be mitigated with a

1

15   positive net present value, although maximum benefit is realized by selectively target-

16   ing larger leaks. Our results show that low-cost leak detection programs can rely on

17   high cost technology, as long as it is applied in a way that allows for rapid detection

18   of large leaks. Any strategy to reduce leakage should require a careful consideration of

19   the differences between low-cost technologies and low-cost programs.

Introduction

21   Fugitive methane (CH_4) emissions from the natural gas system are an important source

22   of anthropogenic greenhouse (GHG) gases,[1] representing $\approx$25% of US CH_4 emissions. In

23   extreme cases, fugitive emissions could offset the climate benefits of switching from other

24   fossil fuels to natural gas.[2,3] Leak detection and repair (LDAR) programs aim to reduce

25   fugitive CH_4 emissions while providing additional revenue to natural gas producers from

26   the sale of recovered gas. LDAR is an area of active research, and many proposed LDAR

27   concepts rely heavily on new technologies, including constant monitoring of gas wells with

28   high precision methane sensors,[4,5] automated surveys of natural gas fields based on IR camera

29   technology,[6] or remote sensing of methane plumes using aircraft or satellites.[7,8]

30   While many LDAR concepts and technologies have been studied in the literature, less

31   work has been performed to rigorously compare different proposed LDAR programs regard-

32   ing their effectiveness. For example, which LDAR technology has the most potential to

33   reduce the cost of CH_4 mitigation? Or, how important is labor minimization in driving cost

34   reductions from a new LDAR concept? Rigorously comparing proposed LDAR programs

35   requires a model of leakage from a gas facility, as well as a model of how an LDAR program

36   would detect any given leak. Such a model must be able to accurately simulate the evolution

37   of leakage through time under various proposed and implemented LDAR programs. This

38   model must also include all major costs of LDAR programs, such as labor and technology

39   costs. Because no such model currently exists, we developed the *Fugitive Emissions Abate-*

40   *ment Simulation Toolkit* (FEAST) model to explore the effect of various LDAR programs

41 on long-term leakage rates.

42 In FEAST, CH_4 leaks in a computer-simulated gas field are generated dynamically as

43 the simulation proceeds. Depending on the LDAR program under study, the repair rate is

44 calculated using a physics-based model: the concentration of methane downwind of every

45 leak is simulated using a Gaussian plume model, and the specifications of a particular LDAR

46 program are applied to the simulated plume to determine whether or not it is detected.

47 LDAR programs in FEAST are represented by a combination of technology parameters

48 (e.g., survey sensitivity) and implementation parameters (e.g., survey frequency). Given an

49 LDAR program, FEAST finds and fixes leaks appropriately. Integrating the leakage rate

50 through time yields the total amount of lost gas under a particular LDAR program. By

51 assigning a value to the lost gas and estimating the cost of maintaining the LDAR program,

52 FEAST estimates the economic value of the LDAR program in net present value (NPV)

53 terms and LDAR program environmental benefits.

54 In this paper, FEAST is applied to four conceptual LDAR programs. We first describe the

55 FEAST methodology and LDAR program representations. We then compare our simplified

56 LDAR programs to illustrate their strengths, weaknesses, potential for improvement and

57 relative value. We conclude with a description of future directions for research.

Methodology

59 FEAST is an open-source model programmed in the MATLAB computing environment.[9]

60 FEAST model code and documentation are made open source as supporting information

61 (SI), and so can be downloaded and used as desired by the reader.

Markov model

63 FEAST simulates leakage from a natural gas field by modeling every potential leaking com-

64 ponent in the field using a two-state Markov process: a component may either be in the

65 "leaking" state or in the "robust" state. The simulation time period is broken into discrete

66 time steps, and every component, whether leaking or not, is given a probability of changing

67 state in a given time step. This probability depends on the LDAR program being simulated

68 and the behavior of the natural gas infrastructure. Note that Markov processes (by defi-

69 nition) do not depend on behavior history, while in reality there is some evidence that the

70 probability of leakage from a component depends on its type and age.[10–13] This is consid-

71 ered further in the discussion section. With more experimental and statistical data, future

72 versions of FEAST could be implemented using higher-order Markov chains.

73   The FEAST Markov model is implemented in three basic steps: gas field initialization,

74 dynamic simulation, and results storage (see Figure 1).

Gas field initialization

76 The initial condition is defined by the number and size of leaks distributed throughout the

77 natural gas field, as well as physical characteristics of the gas field that affect the performance

78 of LDAR programs. Physical characteristics include: distance between wells, number of

79 potentially leaking components per well, and area at each wellsite that must be searched for

80 leaks.

81   Several publicly-available datasets exist that characterize the leakage from existing gas

82 fields (Table 1). As shown in Table 1, the Fort Worth air quality study[14] (henceforth

83 FWAQS) offers the largest sample of leaks that is publicly available. We calculate the av-

84 erage number of leaks per well found in the FWAQS (≈ 2) and apply a truncated normal

85 distribution about this average, approximated to the nearest integer, to initialize leaks in

86 FEAST. FEAST then randomly draws the size of each leak from the leaks found in the

87 FWAQS, which have a heavy-tailed size distribution (i.e., lognormal like: large leaks are

88 proportionally more impactful than would be expected in a simple Gaussian size distribu-

89 tion). The result is a randomly generated set of leaks that is statistically similar to the

90 empirical FWAQS data. FEAST can also use other leak size distributions provided informa-

4
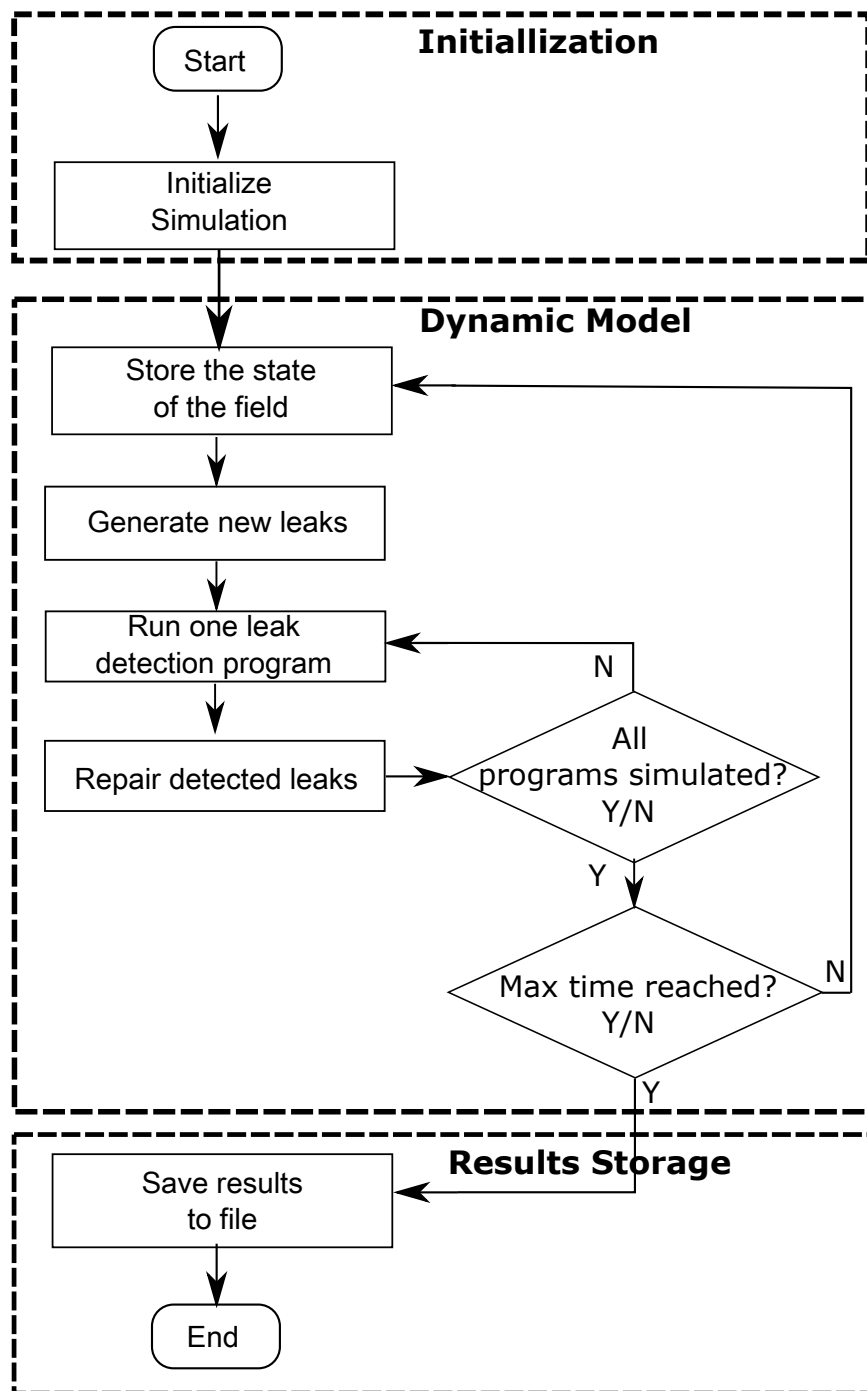
Figure 1: Flowchart of FEAST model structure

91 tion from a user. It should be emphasized here that there is growing evidence [15,16] of highly

92 skewed leak size distribution in the natural gas infrastructure. The leak sizes used in this

93 model, derived from the FWAQS, represents one such heavy-tailed distribution.

94   The distance between wells, number of components per well and other physical features

95 were chosen to be within the range of values found for US natural gas fields (see SI Section

96 S3.2.2, SI Table S3.1).

Table 1: Summary of results from leakage studies of natural gas production facilities

Name	Year	Detection method	Number of wells	Number of leaks	Leaks per well
[a]Carbon Limits[17]	2014	[b]IR camera	≈ 5300	NR	NR
[c]Fort Worth[14]	2011	[d]FID/IR camera	1138	2126[e]	≈ 2
Allen[18] et al.	2013	IR camera	292	769	≈ 2.6
Kuo[19]	2012	Spectroscopy	172	59	≈ 0.3
API 4589[20]	1993	FID	82	1513	≈ 18
Fernandez[11]	2006	Bubble test	12	132	11

a - Carbon Limits reported the number of well sites and well batteries surveyed. We estimate the number of wells by assuming an average of 3 wells per survey in the well sites and well batteries category. There were 39505 leaks recorded in all facilities.
b - Infrared
c - All components were surveyed with an IR camera. 10% were also surveyed with a FID.
d - Flame Ionization Detector
e - Data on the number of wells and leaks can be found in the Government of FortWorth, TX website: http://fortworthtexas.gov/gaswells/air-quality-study/final. Site-specific data can be found in Appendix 3-B: Emissions calculations workbook of the FortWorth, TX Air Quality Study[14]

97 **Atmospheric conditions**

98 The performance of LDAR programs depends on the environmental conditions surrounding

99 the gas field, such as the wind speed and atmospheric stability. The wind speed is chosen

100 from an empirical distribution suggested by ARPA-E in the recent MONITOR challenge.[4]

101 For each time step, one wind speed is selected from this dataset at random. The wind

102 direction is chosen from a second empirical wind dataset collected at Fort Worth.[21] Once the

103 wind speed has been selected, the stability class is chosen at random with equal probability

104 from the realistic classes associated with that wind speed.[22] See SI Section S3.3 for more

105 details. In the absence of site-specific information, the ARPA-E wind speed distribution

106 can be used as a template wind profile near production facilities. Users of this model can

107 input appropriate data sets specific to the infrastructure being studied. It should be noted

108 that meteorological conditions like atmospheric conditions, time of day, etc. can play a

109 significant role in detection capability for different technologies. While these can be included

110 in the technology modeling, the results presented in this paper assume daytime operation

111 for all technologies.

Dynamic simulation

113 At each time step, a small fraction of components in the robust state are changed to the

114 leaking state to emulate a nonzero leak production rate. No published studies were found

115 that directly estimate the leak production rate; however it is possible to use two existing

116 studies to estimate the rate of leak generation.

117 First, the Carbon Limits dataset[17] (henceforth CL) provides one means for estimating

118 the leak production rate. CL reports data from 1000s of wells, suggesting that within the

119 first year after a leak survey is completed the average natural gas well battery emits 1.8

120 tons of volatile organic compounds (tVOC). The associated methane leak creation rate is

121 calculated based on the following four assumptions:

122 • Leakage that persists after the LDAR survey is negligible (i.e., leaks that are found in

123   an LDAR survey are fixed);

124 • The rate of leakage increases linearly throughout the year;

125 • CH_4 and VOC mole fractions are consistent with the average values reported by tech-

126   nical documents;[20]

127 • The number of leaks repaired between LDAR surveys is negligible.

128 Using these assumptions, we derive Equation 1 for the leak creation rate, where E_{VOC} is the

129 estimated total VOC emissions between surveys, Δt is the length of time between surveys

7

130   (one year, in this case) and m_{CH_4}/m_{VOC} is the mass ratio of CH_4 emissions to VOC emissions

131   (see SI section SA.2 for the method used to estimate m_{CH_4}/m_{VOC}). According to Equation

132   1, the CL data suggest a leak creation rate of 3.8×10^{-4} g CH_4/s per well per day.

$$R_l = \frac{2E_{VOC}}{\Delta t^2} \frac{m_{CH_4}}{m_{VOC}} \tag{1}$$

133   Alternatively, FWAQS data[14] can be used to estimate the leak production rate. Based

134   on the assumption that the rate of leakage increased linearly from zero when the facility was

135   first built, the leak creation rate in the Barnett shale region can be estimated by dividing

136   the total leakage rate in the FWAQS study by the average age of gas wells. This gives a

137   leak production rate of 1.8×10^{-4} g/s per well per day, or $\approx 50\%$ of the CL value. FEAST

138   defaults to the average value of 2.6×10^{-4} g/s per well per day. There are many possible

139   explanations for the discrepancy between the two results reported above, including different

140   types of infrastructure, different facility age, different regulations, or different management

141   practices in the two regions studied. As noted below, more work is needed to generate better

142   estimates of the leak detection rate. In order to compensate for the lack of reliable data on

143   leak production rates across the US infrastructure, we have used a range from 1.8×10^{-4} to

144   3.8×10^{-4} g/s per well per day in the sensitivity analysis. Since the model is open source,

145   these values could be replaced with a more representative generation rate for a particular

146   set of gas wells.

147   The probability of a component switching from the robust to the leaking state during a

148   time step of duration δt is given by Equation 2. R_l is the leakage creation rate [g/s per well

149   per day], $N_{c/w}$ is the number of components per well, and μ_l is the average leak size [g/s].

$$P_{R,L} = \frac{R_l}{N_{c/w}\mu_l}\delta t. \tag{2}$$

150   At each time step every robust component is given the probability $P_{R,L}$ to begin leaking.

151   Components that begin leaking have leakage rates drawn from FWAQS empirical data, as

152 during initialization.

153   Choosing a $P_{L,R}$ that is constant through time implies that the quality of gas infrastruc-

154 ture and maintenance does not change during the simulation. It does not imply that the

155 leakage increases linearly through time. On the contrary, the stochastic nature of FEAST

156 allows for a different number of leaks to be introduced at every time step and the size of each

157 created leak is chosen randomly, independent of $P_{L,R}$. Super emitters are extremely large but

158 rare leaks in the FWAQS, and their frequency in FEAST follows the FWAQS distribution.

159 When FEAST happens to generate a super emitter, a significant discontinuity occurs in the

160 total field leakage, just as the total leakage from a real gas field suddenly increases if a tank

161 hatch cover is accidentally left open. Over sufficiently long time scales, these discontinuities

162 can be averaged out and the total leakage will increase approximately linearly if $P_{L,R}$ is

163 constant (and repairs are neglected). A small modification to the Markov model can allow

164 for a variable $P_{L,R}$ if a change in the leak production rate is expected. We explore one such

165 scenario in the discussion section.

166 ## LDAR programs

167 An LDAR program in FEAST includes the combination of an applied LDAR *technology* and

168 an LDAR *implementation*. Technology parameters include factors such as detector costs and

169 sensitivities, while implementation parameters include factors such as frequency of surveys

170 or repair practices. The probability that a leaking component switches to the robust state

171 $(P_{L,R})$ in a given time step requires a model of the LDAR program being evaluated. By

172 definition,

$$P_{L,R} = P_{L,R}^{Null} + P_{L,R}^{LDAR} \tag{3}$$

173 By default, all LDAR simulations include a "Null LDAR program" which contributes $P_{L,R}^{Null}$

174 to the probability of detecting a leak. In the scenarios below, $P_{L,R}^{Null} N_L^i = P_{R,L} N_R^i$, where N_L^i

175 and N_R^i are the initial number of leaking and robust components, respectively. That is, the

176 background rate of leak creation multiplied by the number of robust components equals the

177 rate of leak detection multiplied by the number of leaking components without LDAR, and

178 therefore the number of leaks is in steady state over long-time Markov simulation. Adding an

179 LDAR program on top of the Null program increases the value of $P_{L,R}$ by adding additional

180 probability of finding and fixing leaks $P_{L,R}^{LDAR}$, such that a new, lower steady state leakage rate

181 is reached. Changing the settings of the Null program allows the user to explore scenarios

182 in which the background prevalence of leaks increases as the facility ages (i.e., $P_{L,R}^{Null} N_L^i <$

183 $P_{R,L} N_R^i$).

184 Four simplified example LDAR programs are simulated here. These LDAR programs

185 include:

186 • Flame Ionization Detector (FID) - Manual application of a flame ionization detector

187 technology, after which components with a local CH_4 concentration above a threshold

188 are replaced. The FID technology is the "default" first pass detection technology used

189 in many historical studies.

190 • Distributed Detector (DD) - Methane detectors are placed at intervals along the dom-

191 inant downwind direction characteristic of the location and alert repair crews when

192 local concentrations at a detector exceed a threshold detection limit. After leaks are

193 detected, repairs are performed at a set repair interval.

194 • Manual Infrared (MIR) - A manual infrared imaging method, wherein an operator uses

195 an IR camera to visualize methane plumes and tags components to be fixed. A manual

196 IR technique is another very commonly applied LDAR method.

197 • Automated Infrared (AIR) - An automated infrared technique where an infrared-

198 equipped aircraft flies over natural gas sites and detects leaks from their infrared

199 signature. After leaks are detected, images of each leak are sent to repair crews to

200 facilitate repair.

201   The most important parameters for each LDAR program are given in Table 2. See SI

202 Table S3.5 through Table S3.8 for full details of LDAR parameters and default settings for

203 each LDAR program.

204   In the FID survey method, all leaks are found and repaired at each time step when a

205 survey occurs. Therefore, $P_{L,R}^{LDAR} = 0$ at all time steps, except at the time step of a survey

206 when $P_{L,R}^{LDAR} = 1$. Such a detection certainty is justified because the underlying dataset used

207 in FEAST was obtained using a FID-based leak detection program.

208   FEAST uses a Gaussian plume model to compute $P_{L,R}^{LDAR}$ for the DD, MIR, and AIR

209 programs. Such a model accounts for the buoyancy of emitted gas and reflection of the

210 plume off the ground. The effect of an atmospheric inversion is not considered since we

211 are interested in the behavior of plumes within a few tens of meters of the ground. The

212 concentration Φ [g/m³] downwind of the plume is given by,

$$\Phi = \frac{Q}{2\pi u \sigma_y(x) \sigma_z(x)} exp\left(\frac{(y-y_0)^2}{2\sigma_y^2(x)}\right)\left[exp\left(\frac{(z-z_M(x))^2}{2\sigma_z^2(x)}\right) + exp\left(\frac{(z+z_M(x))^2}{2\sigma_z^2(x)}\right)\right] \quad (4)$$

213 where x, y and z are the coordinates at which the concentration is to be calculated [m]:

214 x is measured downwind of the leak, z is the vertical displacement from the ground, y_0 is

215 the position of the leak source in the y direction, Q is the leak flux [g/s] and u is the wind

216 speed [m/s]. σ_y and σ_z are the standard deviation of the plume concentration [m], extracted

217 using linear interpolation to published curves[22–24] based on the atmospheric stability class.

218 Finally, z_M is the vertical position of the middle of the plume as a function of x. z_M accounts

219 for the plume buoyancy and follows the methodology suggested by Beychok (see SI Section

220 S2.3).[25]

221   The DD, MIR and AIR programs use the Gaussian plume model in different ways. For

222 the DD detector, the concentration of methane at the location of the plume is compared to

223 a predefined detection threshold. If the concentration is greater than the threshold, the leak

224 is detected. The probability that the concentration exceeds the detection threshold depends

Table 2: Notable parameter settings in the base case and extreme sensitivity cases. See SI for complete list of Markov model and LDAR program specifications.

Symbol	Name	Units	Base Case	High Savings	Low Savings
Markov Model					
R_l	Leak production rate	g/s-well-day	2.6×10^{-4}	5.2×10^{-4}	1.3×10^{-4}
-	Leak size data source	-	FWAQS [14]	Allen [18]	-
C_g	Gas price	\$/mcf	5	8	3
R_{RD}	Real discount rate	% per y	8	5	10
A	Aging factor	-	1	2	-
FID					
C_{Cap}	Total capital	\$	35000	20000	50000
λ	Lifetime	years	10	5	20
R_S	Survey speed	components/hour	150	300	75
T_{SI}	Survey interval	days	100	50	200
T_{SU}	Setup time	hours	0.5	-	-
DD					
$C_{detector}$	Cost per detector	\$	500	200	1000
$N_{s/W}$	detectors per well	-	4	2	8
T_{LI}	Repair interval	days	50	25	100
T_{setup}	Setup time	hours	0.5	-	-
Φ_{min}	Min. concentration	g/m^3	10^{-2}	10^{-3}	10^{-1}
MIR					
C_{Cap}	Capital cost	\$	120000	60000	240000
λ	Lifetime	years	10	5	20
R_S	Survey speed	components/hour	500	1000	250
Γ_{min}	Min. conc. path.	m-g/m^3	0.4	0.2	2
$F_{PD,min}$	Min. fraction of pixels above Γ_{min} for detection	%	10	5	20
T_{SI}	Survey interval	days	100	50	200
T_{SU}	Setup time	hours	0.5	-	-
AIR					
C_{cap}	Total capital cost	\$	193000	100000	300000
$F_{PD,min}$	Min. fraction of pixels above Γ_{min} for detection	%	10	5	20
Γ_{min}	Min. conc. path.	m-g/m^3	0.4	0.2	2
T_{SI}	Survey interval	d	14	7	28
v_S	Survey speed	m/s	5	10	2.5
Z_{cam}	Camera height	m	20	10	40
λ	Lifetime	y	3	5	1.5

225 on the size of the leak, the location of the leak relative to the detector, and atmospheric

226 conditions. The location of the leaks are chosen randomly within a pad area definition.

227 Various placement patterns of DD sensors are explored in prior work. [26]

228   The detection threshold for the IR camera methods requires that a minimum fraction of

229 the camera pixels be above a minimum concentration pathlength. [27] The signal in each pixel

230 is estimated by numerically integrating the concentration calculated by the Gaussian plume

231 model along the path imaged by each pixel according to Equation 5, where α is an implied

232 constant in the detection criteria and Λ is the path imaged by a pixel.

$$Signal = \alpha \int_{\Lambda} \Phi(x(s), y(s), z(s))ds \tag{5}$$

233   A simulation of this concentration-pathlength, as seen by an IR camera 30 m to the side

234 of the leak source, for two different leak rates, using the Gaussian plume model is shown in

235 Figure 2.
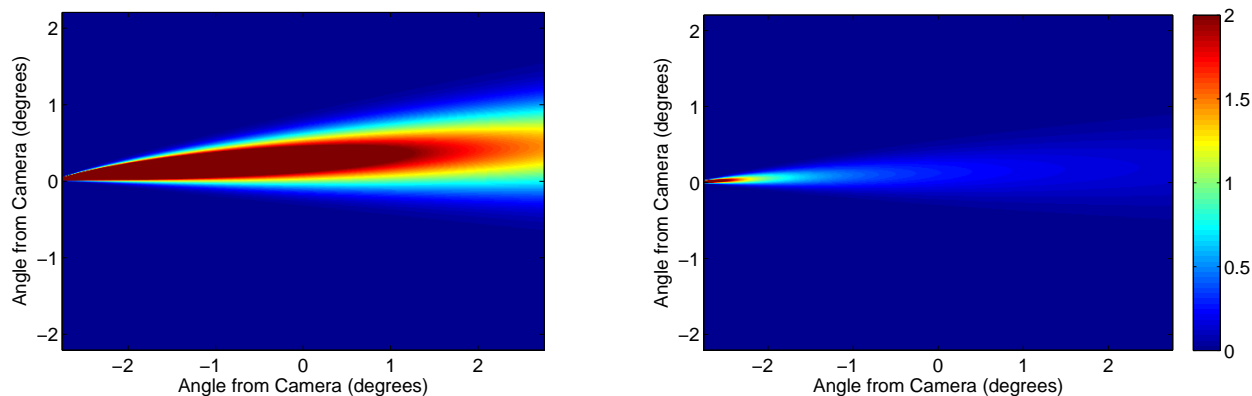
Figure 2: Simulated concentration-pathlength profile of natural gas leaks of 1.5 g/s (left) and 0.15 g/s (right), at a wind speed of 2 m/s and stability class C. Leaks are imaged by a camera 30 meters to the side of the leak source. The color bar indicates the signal to noise ratio as imaged by the IR camera.

Economic analysis

The Markov model generates a time series of leakage associated with each simulated LDAR technology. Assigning a value to the gas saved by an LDAR program in comparison to a status quo simulation (in this case the Null LDAR program) enables an NPV analysis of each modeled LDAR program and an estimate of the CH_4 emitted.

We use a standard NPV analysis to compare the economic value of various LDAR programs. The NPV is calculated according to Equation 6, where $\mathbb{Z}_t$ is the set of all time steps, $V_L(t_i)$ is the value of the leakage lost during the ith time step, and C is the cost of running the LDAR program in the ith time step. R_{RD} is the real discount rate (8%).

$$NPV = \sum_{i \in \mathbb{Z}_t} \left(V_L(t_i) - C(t_i) \right) \left(\frac{1}{1 + R_{RD}} \right)^{t_i} \tag{6}$$

The price of natural-gas for base-case analysis is fixed at \$5/mcf over the entire simulation period, while a range from \$3/mcf to \$8/mcf is used for sensitivity analysis. The cost of fixing leaks is drawn at random from a comprehensive list of over 1600 leaks from a 2006 EPA study,[11] with costs adjusted for inflation. There was no correlation between the measured leak magnitudes in that study and the estimated costs to fix each leak (see SI Fig. S3.14) thereby justifying randomly selecting costs. It should be noted that the NPV analysis performed here is only representative, and is best used as a tool to compare various LDAR technologies in terms of its cost-effectiveness instead of absolute dollar terms. Further refinement of this model would need to incorporate enterprise-level information regarding captial structures and specific characteristics of the business model in use.

Results and discussion

A FEAST scenario is defined by the user defined settings, inputs and the underlying dataset provided to FEAST. We refer to the results generated by running FEAST once as one

258 *realization* of a particular scenario. Because FEAST is stochastic, results will change each

259 time FEAST runs a particular scenario. Numerous realizations must be analyzed in order

260 to understand the the implications of a particular scenario.

261 Figure 3 shows the leakage time series of a single realization of the default scenario in

262 FEAST for different LDAR programs, including the Null program and a No-Repair program.

263 While the time-series change in total leakage will be different for each realization because of

264 the stochastic nature of the model, the general trends in Figure 3 are characteristic of the

265 LDAR programs. This simulation covers a 10-year time period, so the number of evaluation

266 periods is large and steady-state behavior is always reached. The gas saved over the duration

267 of the simulation by a particular LDAR program is the area between the Null program time

268 series and the LDAR program time series.

269 The Null LDAR program is intended to emulate repairs that occur in the field without

270 any explicit LDAR program, and is set in this scenario as noted above ($P_{L,R}N_L^i = P_{R,L}N_R^i$).

271 These Null program repairs may occur during routine maintenance or upgrades to equipment.

272 We suggest that the Null program be used to represent the status quo, although users can

273 choose their own baseline. The No-Repair program never removes any leaks from the gas

274 field, and the leakage increases indefinitely ($P_{L,R} = 0$). Because the Null scenario repairs the

275 majority of the leaks compared to a No-Repair scenario, it is only instructive to compare

276 any marginal-advantages of an LDAR program to the Null scenario (i.e., No-Repair results

277 are not used to calculate LDAR benefits below).

278 There are two types of variability in FEAST: the variability in the mean behavior between

279 different scenarios and the stochastic variability between realizations. Figure 4 illustrates

280 both of these types of variability. The left figure shows the difference in the mean behavior

281 of the LDAR programs, broken down into cost and benefit components. We can see that

282 the labor cost (a major component of "Finding Cost") dominates in some technologies (e.g.,

283 FID), while the capital cost dominates in others (e.g., DD). The error bars represent the

284 standard error in the estimate of the mean due to the limited sample size employed here.
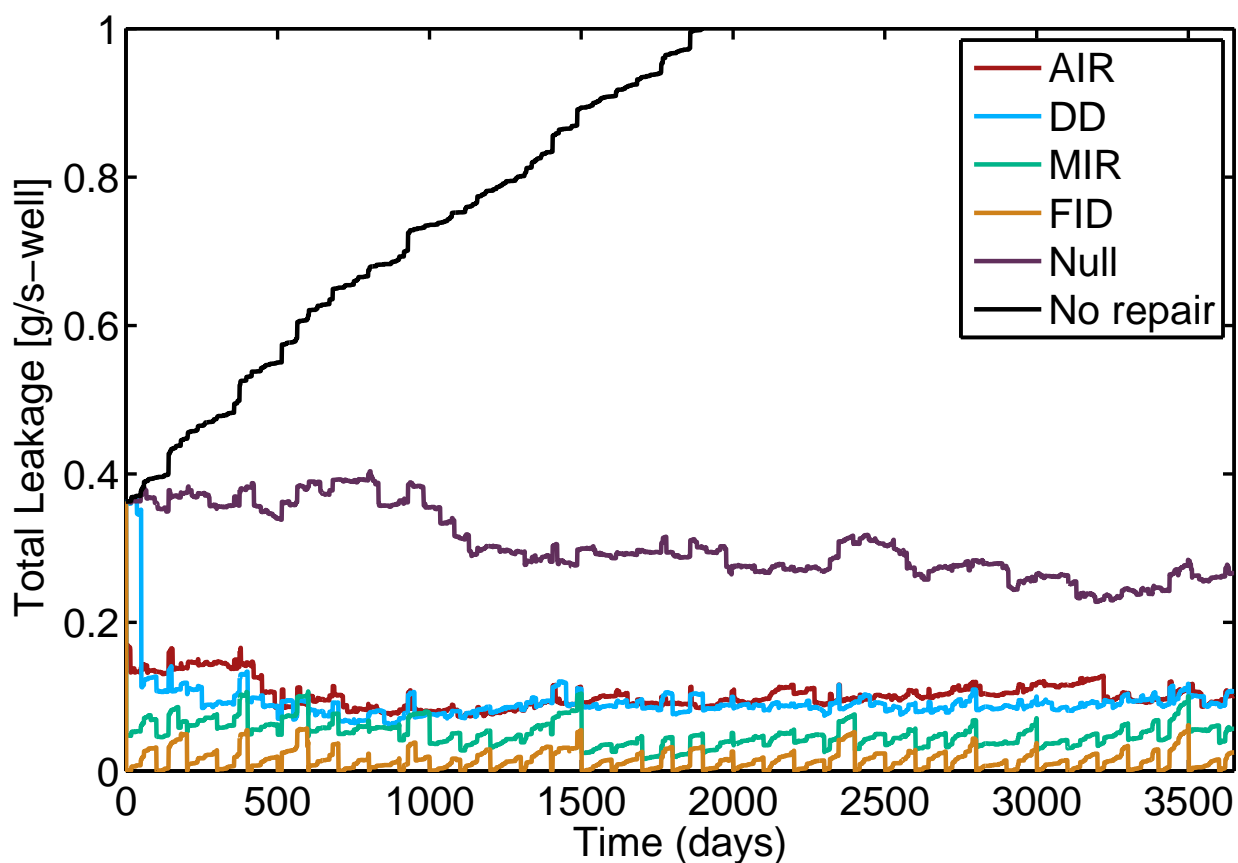
Figure 3: Time series of a single realization of the default scenario in FEAST for the four different LDAR programs, including the null and no-repair program. In the no-repair case, the total leakage doubles within a few years, while it reaches a steady state in every other case. The null repair scenarios fixes the majority of the leaks compared to the no-repair scenario, and therefore any marginal-advantage of the LDAR programs are calculated when compared to the null scenario.

285   The standard error was computed as:

$$\sigma_\mu = \frac{\sigma_s}{\sqrt{N}} \tag{7}$$

286   where σ_μ is the population mean, σ_s is the sample mean, and N is the number of samples

287   (realizations). In this work, $N = 100$ for each scenario. The variation between stochastic

288   realizations is shown in the right side of Figure 4. We see that while the variation between

289   realizations is large, the technologies are different enough that clear trends can be discerned.

290   Considering the median NPV for all realizations, the AIR, DD and MIR LDAR programs

291   have a positive NPV across the range of inter-realization variability. Compared with these

292   technologies, the intensive labor costs for an FID-based LDAR program results in a negative

293   median NPV.
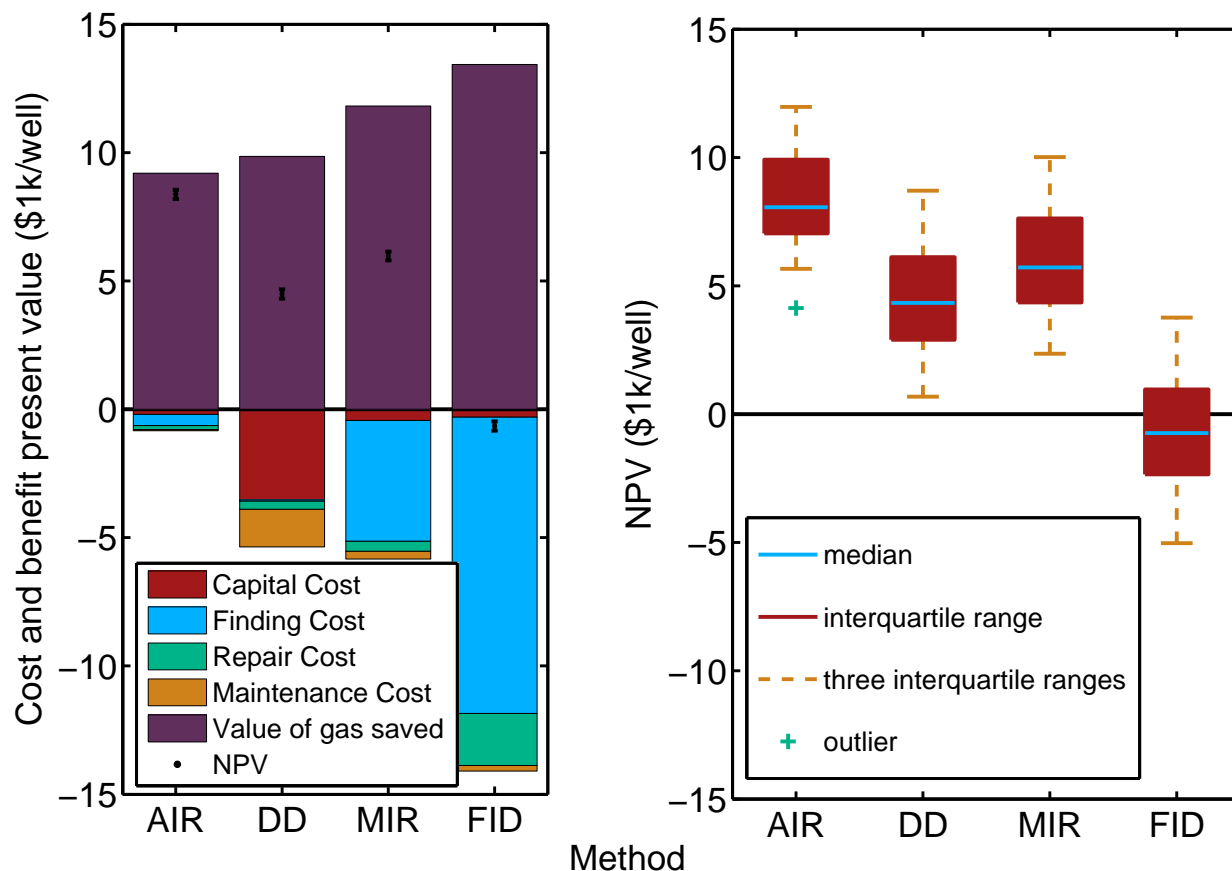
Figure 4: (left) Variability in the mean behavior between different scenarios of the various LDAR programs shown as a cost vs benefit diagram. Note that the distribution of costs between capital, labor, repairs and maintenance are dependent on the technology and the methodology adopted in the LDAR program. For example, while the cost of implementing a DD program is dominated by the cost of the detectors, the FID program effectively depends only on labor costs. (right) Stochastic variability between different realizations of a scenario for different LDAR programs. While the variation exceeds 50% of mean in some cases, clear trends can be observed: the FID program, highly dependent on labor cost, has a significantly lower NPV compared to other LDAR programs.

294   Perhaps the most instructive results from FEAST are illustrated by varying scenario

295   settings, as shown in a tornado diagram in Figure 5. The settings used to generate these

296   sensitivity cases are given in Table 2. They were chosen to represent the realistic range of

297   values for each parameter. Note that simulating fields within the realistic range of leak pro-

298   duction rates given available data results in enormous variability between scenarios. Clearly,

299   improved data to quantify the leak production rate of gas fields would mitigate the primary

300 driver of uncertainty in FEAST.

301   One of the base case assumptions in FEAST is a constant leak production rate. Some

302 evidence suggests that gas infrastructure is likely to produce leaks at a greater rate as it

303 ages, although little data exist to quantify this effect in natural gas wells.[10–13] We allow for

304 a variable leak production rate in one sensitivity case: the leak production rate increase

305 linearly from 2.6×10^{-5} g/s per well per day to twice its value over the 10 year simulation

306 period. It can be clearly seen from Figure 5 that any additional increase in the baseline leak

307 creation rate only increases the value of the LDAR programs.
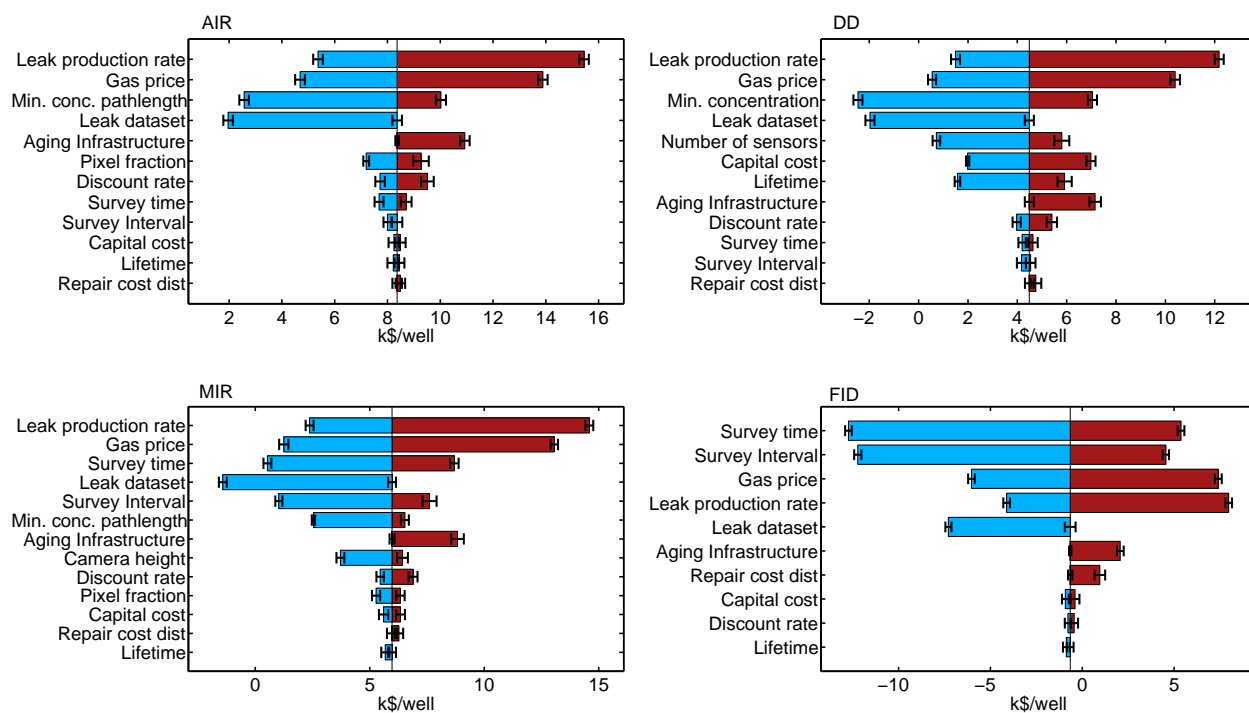
Figure 5: Sensitivity of the NPV of the four simulated LDAR programs to various parameters of the natural gas field, detection technology and survey procedures. It should be noted that extrinsic factors like the leak production rate and gas price play an out-sized role in determining the NPV of various LDAR programs. In the case of FID, which has significantly lower NPV than other LDAR programs, we see that reducing the intervals of leak detection will result in a greater cost reduction compared to the reduction in gas savings.

308   Each LDAR program has unique characteristics that can be adjusted in FEAST to explore

309 their effects. The FID program can be greatly improved by reducing the time required to

310 complete surveys and decreasing the frequency of surveys from the default case. This is

311 because the baseline FID cost is dominated by the labor cost of this slow technology. This

312 result is intuitive because the FID program has no trouble finding leaks and labor is the

313 primary cost of the FID program; reducing the frequency of surveys reduces labor costs

314 more than it decreases gas savings.

315 In either IR camera program, improving the sensitivity of each camera pixel to methane

316 increases the value of the LDAR programs. However, the results are less sensitive to the

317 number of pixels that must be above the detection limit. Only the MIR program is sensitive

318 to the survey time and survey interval of the program, while the value of the AIR program is

319 largely independent of these factors. In fact, the AIR program is only sensitive to properties

320 that affect the number and size of leaks that it detects. This is because the amortized

321 operating costs of the AIR program are very small in comparison to the amount of gas that

322 it detects, due to the fact that the automated airborne system can visit a large number of

323 wells per unit time. Reducing the amount of gas detected by 20% has a greater effect on the

324 cash flow of the AIR program than doubling its operating expenses.

325 The DD program shares many traits with the AIR program: it benefits from changes that

326 increase the number of leaks detected and is insensitive to the survey interval and survey time

327 required to pinpoint the location of leaks. However, the distributed detector program is the

328 only program simulated that is significantly sensitive to the capital cost of the equipment.

329 A distributed detector program requires detectors to be placed at every well, while a single

330 piece of survey equipment for an FID, MIR or AIR program can service hundreds or even

331 thousands of gas wells, depending on the survey frequency and time for each survey. Low

332 sensitivity methane detectors can have extremely low capital costs on the order of $1, but

333 detectors with ppb scale sensitivity can cost $10,000 to $100,000. In the base case, we

334 simulated an intermediate detector with a cost of $500 and a sensitivity of 15 ppm.

335 Notwithstanding the sources of variability in results outlined above, the absolute values

336 computed with FEAST are encouraging. We found that the MIR, AIR, and DD programs

337 are likely to have positive NPVs. Under most scenarios we considered, the AIR program has

338   the greatest NPV, ranging up to $15,000$ per well over a ten year period in the best case

339   sensitivity scenario (see Figure 5).

340   The most speculative of these scenarios is perhaps the AIR program. Some AIR assump-

341   tions may ultimately prove unrealistic. However, the basic characteristics of the program

342   that make it cost effective are instructive: it allows for high speed servicing of wells and only

343   identifies relatively large leaks. Sacrificing some sensitivity for speed allows the majority of

344   leakage to be found (when using realistic heavy-tailed leak size distributions) while greatly

345   reducing operating costs and reducing the cost of fixing small leaks with small gas savings.

346   With these factors included, the capital cost of a drone and high performance IR camera

347   system (estimated at $193k for the purposes of this example) proved to be largely immate-

348   rial to the project NPV. This clearly shows that there is a significant divergence between

349   low-cost LDAR *technologies* ("cheap detectors") and low-cost LDAR *programs* ("cheap de-

350   tection"). Low-cost LDAR programs can in fact rely on highly sophisticated and high cost

351   technology, as long as this technology is applied in a way that allows for rapid scanning and

352   robust detection of large leaks. The end-member of such a technology spectrum would be a

353   high-resolution satellite-based system, which would have very high capital costs, but could

354   in principle detect leaks across a wide swath of the Earth's surface each day.

355   One of the big challenges in the methane leakage problem is its magnitude - the vast

356   variety in the infrastructure and skewed leak size distribution makes direct measurements

357   and subsequent extrapolation costly (i.e. large sample sizes are needed). Considering the

358   costs associated with implementing leak detection programs, it becomes vitally important to

359   develop tools to help businesses develop cost effective strategies. FEAST is general enough

360   to allow businesses and others to tailor the model to specific sites/conditions as they see fit.

361   The results presented here should not be taken as definitive but more as an example of the

362   various possibilities available to users

363   We emphasize that the economic analysis of various LDAR programs presented here is

364   only indicative of general trends, and should not be interpreted as a definitive analysis of

the cost-benefits ratio for a given technology. Also, FEAST NPV calculations are operator-centric: they take into account the additional revenue from the sale of recovered gas in its cost-benefit analysis, but neglect other important effects such as the social cost of carbon, a future carbon tax or carbon trading market, health benefits associated with the reduction of Volatile Organic Compounds (VOCs) and the avoided costs of climate change adaptation. In proposing new regulations to reduce methane emissions from the US oil and natural gas industry by 40 to 45% from 2012 levels in 2025, the Environmental Protection Agency (EPA) has estimated net climate benefits alone at \$120 million to \$150 million.[28] Adding benefits accrued from reductions in health effects related to fine particle pollution, ozone, air-toxics, and improvements in visibility would only incentivize support for a strong methane mitigation policy, resulting in a much higher social NPV for various LDAR programs.

Supporting Information Available

Simulation code in MATLAB along with supporting technical documentation and user-guide This material is available free of charge via the Internet at `http://pubs.acs.org/`.

References

(1) *Inventory of U.S. Greenhouse Gas Emissions and Sinks: 1990-2012*; U.S. Environmental Protection Agency: Washington, DC. 2014.

(2) Alvarez, R. A.; Pacala, S. W.; Winebrake, J. J.; Chameides, W. L.; Hamburg, S. P. Greater focus needed on methane leakage from natural gas infrastructure. *Proceedings of the National Academy of Sciences* **2012**, *109*, 6435–6440.

(3) Brandt, A.; Heath, G. A.; Kort, E. A.; O'Sullivan, F.; Petron, G.; Jordaan, S. M.; Tans, P.; Wilcox, J.; Gopstein, A. M.; Arent, D.; Wofsy, S.; Brown, N. J.; Bradley, R.;

Stucky, G. D. Methane Leaks from North American Natural Gas Systems. *Science* **2014**, *343*, 733–735.

(4) Methane Observation Networks with Innovative Technology to Obtain Reductions – MONITOR. 2014; `http://arpa-e.energy.gov/sites/default/files/documents/` `files/MONITORandDELTAProjectDescriptions_Final_12.15.14.pdf`.

(5) Methane Detectors Challenge. 2015; `https://www.edf.org/energy/` `natural-gas-policy/methane-detectors-challenge`.

(6) *Rebellion Photonics*. 2015; `http://rebellionphotonics.com/`.

(7) Kort, E.; Frankenberg, C.; Costigan, K. R.; Lindenmaier, R.; Dubey, M. K.; Wunch, D. Four corners: The largest US methane anomaly viewed from space. *Geophysical Research Letters* **2014**, *41*, 6898–6903.

(8) KairosAerospace. `http://kairosaerospace.com/`.

(9) Mathworks Inc., MATLAB v. 2015b. 2015.

(10) Gallagher, M. E.; Down, A.; Ackley, R. C.; Zhao, K.; Phillips, N.; Jackson, R. B. Natural Gas Pipeline Replacement Programs Reduce Methane Leaks and Improve Consumer Safety. *Environmental Science and Technology Letters* **2015**, *2*, 286–291.

(11) Fernandez, R. *Cost Effective Directed Inspection and Maintenance Control Opportunities at Five Gas Processing Plants and Upstream Gathering Compressor Stations and Well Sites*; Environmental Protection Agency: Washington, DC. 2006.

(12) Jackson, R. B.; Down, A.; Phillips, N. G.; Ackley, R. C.; Cook, C. W.; Plata, D. L.; Zhao, K. Natural gas pipeline leaks across Washington, DC. *Environmental science & technology* **2014**, *48*, 2051–8.

409   (13) Phillips, N. G.; Ackley, R.; Crosson, E. R.; Down, A.; Hutyra, L. R.; Brondfield, M.;
410   Karr, J. D.; Zhao, K.; Jackson, R. B. Mapping urban pipeline leaks: Methane leaks
411   across Boston. *Environmental Pollution* **2013**, *173*, 1–4.

412   (14) *City of Fort Worth Natural Gas Air Quality Study*; City of Fort Worth: Fort Worth,
413   TX. 2011; `http://fortworthtexas.gov/gaswells/air-quality-study/final/`.

414   (15) Lyon, D. R.; Zavala-Araiza, D.; Alvarez, R. A.; Harriss, R.; Palacios, V.; Lan, X.;
415   Talbot, R.; Lavoie, T.; Shepson, P.; Yacovitch, T. I.; et. al, Constructing a spatially re-
416   solved methane emission inventory for the Barnett Shale region. *Environmental science*
417   *& technology* **2015**, *49*, 8147–8157.

418   (16) Brandt, a. R. et al. Energy and environment. Methane leaks from North American
419   natural gas systems. *Science (New York, N.Y.)* **2014**, *343*, 733–5.

420   (17) Saunier, S. Quantifying Cost-effectiveness of Systematic Leak Detection and Repair
421   Programs Using Infrared Cameras; Carbon Limits: Oslo, Norway. 2014; `http://www.`
422   `carbonlimits.no/PDF/Carbon{\_}Limits{\_}LDAR.pdf`.

423   (18) Allen, D.; Torres, V. M.; Thomas, J.; Sullivan, D. W.; Harrison, M.; Hendler, A.;
424   Herndon, S. C.; Kolb, C. E.; Fraser, M. P.; Hill, A. D.; Lamb, B.; Miskimins, J.;
425   Sawyer, R.; Seinfeld, J. Measurements of methane emissions at natural gas production
426   sites in the United States David. *Proceedings of the National Academy of Sciences* **2013**,
427   *110*, 18025–18030.

428   (19) Kuo, J. *Estimation of methane emissions from the California Natural Gas System*;
429   California Energy Commission: Fullerton, CA. 2012; `http://www.energy.ca.gov/`
430   `2014publications/CEC-500-2014-072/CEC-500-2014-072.pdf`.

431   (20) Bourke, J.; Mire, K.; Newsom, V.; Pike, M.; Ramanan, R.; Shah, A.; Strong, J.; Tix-
432   ier, C.; Yang, J. *Fugitive Hydrocarbon Emissions from Oil and Gas Production Opera-*
433   *tions*; American Petroleum Institute, Publ. No. 4589: Washinton, DC. 1993.

434 (21) NOAA National Weather Service Forecast Office Dallas/FortWorth, TX Climate Data.

435   2014; `http://www.srh.noaa.gov/fwd/?n=dfwclimo`.

436 (22) Seinfeld, J.; Pandis, S. *Atmospheric Chemistry and Physics*, 2nd ed.; Wiley and Sons,

437   Inc: Hoboken, NJ, 2006.

438 (23) Pasquill, F. The estimation of the dispersion of windborne material. *The Meteorological*

439   *Magazine* **1961**, *90*, 33–49.

440 (24) Gifford, F. A. Use of Routine Meteorological Observations for Estimating Atmospheric

441   Dispersion. *Nuclear Safety* **1961**, *2*, 47–51.

442 (25) Beychock, M. *Fundamentals of Stack Gas Dispersion*, 4th ed.; 2005.

443 (26) Kemp, C. A Simulation Method for Methane Leak Detection and Repair Technologies.

444   Master's Thesis, Stanford University, Stanford, CA, 2015.

445 (27) Benson, R. G.; Panek, J. A.; Drayton, P. Direct Measurements of Minimum Detectable

446   Vapor Concentrations Using Passive Infrared Optical Imaging Systems. Paper 1025 of

447   Proceedings 101st ACE meeting (held June 2008 in Portland, Oregon) of the Air and

448   Waste Management Association. 2008.

449 (28) Oil and Natural Gas Sector: Emission Standards for New and Modified Sources. *Federal*

450   *Register* **2015**, *80*, 56593.

451 # Graphical TOC Entry

452

Dynamic leak creation and detection